

Effect of contact potential barrier of organic resists on atomic force microscope anodization lithography

Jeong Oh Kim, Wansup Shin, Hyeyoung Park, Haiwon Lee*

Department of Chemistry, Hanyang University, Haengdang-dong, Sungdong-gu, Seoul 133-791, Republic of Korea

Available online 15 December 2004

Abstract

The local oxidation on Si substrate has been studied by atomic force microscope lithography. Heights of protruded patterns were changed during the lithographic process with thin films of 2-amino-6-methoxybenzothiazole-azo (MBT-A) and 2-amino-6-methoxybenzothiazol-azo-Ni ($[\text{MBT-A}]_2\text{Ni}^{2+}$) on Si substrates. The current-value in a tip-sample junction was investigated by using scanning tunneling spectroscopy with a contact mode atomic force microscope (AFM), and it was confirmed that a change of current-values depends on applied voltages. The difference of potential barrier between $[\text{MBT-A}]_2\text{Ni}^{2+}$ and MBT-A was also confirmed by using UV-vis spectrophotometry and ultraviolet photoelectron spectroscopy. The tunneling current value of a $[\text{MBT-A}]_2\text{Ni}^{2+}$ film was larger than that of MBT-A film and the difference from threshold voltages was also observed.

© 2004 Elsevier B.V. All rights reserved.

Keywords: AFM lithography; *I*-*V* curve; Scanning tunneling spectroscopy; Contact potential barrier; Fermi energy level

1. Introduction

Many nanolithographic methods have been developed to overcome 100 nm limit of the line width, and those methods are such as electron-beam lithography [1], imprint lithography [2], and scanning probe microscope (SPM) lithography [3]. Among the several patterning techniques, SPM lithography is a very promising technique with regard to ease in obtaining high-resolution patterns. While fabricating a nanostructure is rather difficult on semiconductor materials by using scanning tunneling microscope (STM) lithography, the atomic force microscope (AFM) anodization lithography is effectively applied to obtain patterns on semiconductor and metal substrates. However, because of the slow lithographic scanning speed and the weariness of an AFM tip, the application to a large area is still limited. Recently our group has reported that the speed of lithographic writing can be improved dramatically with highly sensitive organic resists [4,5]. Since the property of organic resist can be modified by incorporating a functional group into the structure of molecular resists,

the property change of organic resists contributes to develop a better resist for fabricating nanostructures on various substrates at the high speed of lithographic writing. For example, the lithographic scanning speed was dramatically enhanced by the addition of an electron-accepting group to the main structure of an organic resist [6]. Furthermore, by changing the polarity of applied voltage on Langmuir-Blodgett monolayer on a silicone substrate, either positive or negative patterns were successfully fabricated [7,8]. In general, in AFM anodization lithography using organic resists, the line width and the height of protruding patterns were very much affected by various lithographic factors such as lithographic speed [9], magnitude of bias [9], humidity [10], surface group [11], etc.

The AFM anodization lithography is performed by a capillary phenomenon of absorbed water and Faradaic current attributed to the transport of OH^- ions [12]. According to the mechanism of anodization lithography, the OH^- ions are related to the electron migration through the tip-sample junction. Generally, the tunneling current can be measured by scanning tunneling spectroscopy (STS) mode [13,14]. If the real current value of anodization AFM lithography is known, the height of protruding lines can be controlled by adjusting the amount of total current between the tip and

* Corresponding author. Tel.: +82 2 2290 0945; fax: +82 2 2296 0287.
E-mail address: haiwon@hanyang.ac.kr (H. Lee).

the sample. Organic materials that have intrinsic Fermi energy levels showed specific I - V curves [15]. In this study, 2-amino-6-methoxybenzothiazole-azo (MBT-A) and 2-amino-6-methoxybenzothiazol-azo-Ni ($[\text{MBT-A}]_2\text{Ni}^{2+}$) were investigated. As both azo dye and metal-azo dye showed maximum absorption peaks at different wavelengths, these materials have different energy band gaps, respectively [16]. In order to investigate the electrical property of resists, the current measurement was performed in situ during AFM anodization lithography.

2. Experiment

The n-type Si(100) wafers with a resistivity of 18–21 Ω cm (LG Siltron Co., Korea) used as substrates for spin-coating the organic materials. The organic contaminants on Si wafers were removed by ultrasonic cleaning in acetone and isopropyl alcohol before use and wafers were dried by N_2 blow. The 2-amino-6-methoxybenzothiazole-azo (MBT-A) and 2-amino-6-methoxybenzothiazol-azo-Ni ($[\text{MBT-A}]_2\text{Ni}^{2+}$) were synthesized to use as resists [16]. Because of fabrication of standard film thickness, 6 mM of MBT-A and 1 mM of $[\text{MBT-A}]_2\text{Ni}^{2+}$ solutions in ethanol were prepared and these organic solutions were spin-casted onto a silicon substrate at the speed of 3000 rpm for 30 s. De-ionized water purified with Milli-Q (18 M Ω cm resistivity, Millipore, USA) was used. The average thickness and uniformity of the film were measured by an ellipsometer (Auto EL II, Rudolph Technology Inc., USA). The HOMO levels of MBT-A and $[\text{MBT-A}]_2\text{Ni}^{2+}$ films were measured using ultraviolet photoelectron spectroscopy (UPS). Apparatus is ESCALAB 220 (Thermo VG Scientific) with the base pressure of 10^{-10} Torr. A UV light (He $I=21.22$ eV) was used as the excitation source. UV-vis spectra were recorded with films on a quartz plate coated by using 6 mM of MBT-A and 1 mM of $[\text{MBT-A}]_2\text{Ni}^{2+}$ solutions using a Scinco spectrophotometer. A tip used in this experiment was a Pt-coated silicon tip (Micro Masch, Russia) with a force constant of 0.6 N/m. All lithographic, imaging process, and scanning tunneling spectroscopy (STS) measurements were performed using a P-47 Solver (NT-MDT, Russia) under ambient air condition. All of anodization processes were performed at the same lithographic speed of 10 $\mu\text{m/s}$ and relative humidity during the experiment was about 50%.

3. Results and discussion

Because the measurement of I - V curves was largely affected by tip-sample distance [17,18]. The uniformity of the thickness of MBT-A and $[\text{MBT-A}]_2\text{Ni}^{2+}$ films was important, and thin films with the thickness of 25 ± 2 \AA were prepared by a spin-casting method. Root mean square (RMS) roughness of MBT-A and $[\text{MBT-A}]_2\text{Ni}^{2+}$ films were 0.24 and 0.18 nm, respectively.

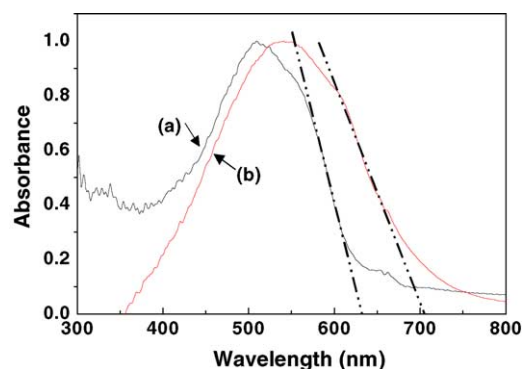


Fig. 1. UV-vis spectra of (a) MBT-A and (b) $[\text{MBT-A}]_2\text{Ni}^{2+}$ films on quartz plate.

Fig. 1 shows UV-vis spectra of MBT-A and $[\text{MBT-A}]_2\text{Ni}^{2+}$ films. Because of the substituent group of MBT-A and Ni ion, the absorption peak of $[\text{MBT-A}]_2\text{Ni}^{2+}$ film was observed at the longer wavelength. The energy band gaps of MBT-A and $[\text{MBT-A}]_2\text{Ni}^{2+}$ films are 1.98 and 1.71 eV, respectively.

Fig. 2(a) and (b) show a change of intensity on MBT-A and $[\text{MBT-A}]_2\text{Ni}^{2+}$ films with binding energy measured by using UPS. The Fermi energy levels can be simply calculated

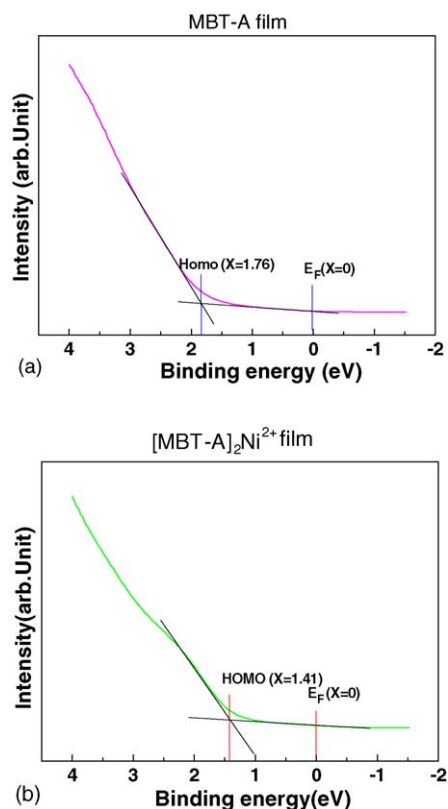


Fig. 2. UPS spectra of (a) MBT-A and (b) $[\text{MBT-A}]_2\text{Ni}^{2+}$ films on Si substrates.

using the formula of [19]:

$$E_F = h\nu - E_{kin}(h\nu, x) \tag{1}$$

where E_F is the Fermi energy level of organic resists, $h\nu$ is line sources of energy 21.21 eV (He I), and $E_{kin}(h\nu, x)$ is a binding energy of level x . The HOMO levels of MBT-A and $[\text{MBT-A}]_2\text{Ni}^{2+}$ films are 5.56 and 5.27 eV, respectively. Moreover, the LUMO levels of MBT-A and $[\text{MBT-A}]_2\text{Ni}^{2+}$ films from the UV–vis spectra are 3.58 and 3.56 eV, respectively.

Fig. 3 shows a schematic band diagram of organic resists used in AFM lithography. When a tip contacts with organic resists, the migration of ion or electron charge is occurred followed by achieving the equilibrium of Fermi energy level between the tip and organic resists. And then, the contact potential barrier (V_0) is formed. The contact potential is the difference from the Fermi level between a tip and an organic resist ($\Phi_m - E_F$). It can be simply calculated using the formula of [20]:

$$V_0 = \Phi_m - E_F \tag{2}$$

where Φ_m is a work function value of Pt metal tip (5.65 eV) and E_F is the Fermi level of organic resists. From the formula (2), the V_0 of MBT-A and $[\text{MBT-A}]_2\text{Ni}^{2+}$ films are determined as 1.84 and 1.79 eV, respectively. Each of organic resists has an intrinsic Fermi level. The lithographic threshold voltages of MBT-A and $[\text{MBT-A}]_2\text{Ni}^{2+}$ films were 4 and 3 V, respectively. The protruded lines on MBT-A film were a width of 87 ± 8 nm and a height of 0.3 ± 0.1 nm. And, the protruded lines on $[\text{MBT-A}]_2\text{Ni}^{2+}$ film had a width of 82 ± 3 nm and a height of 0.3 ± 0.1 nm.

Fig. 4 shows the change of current with lithographic distance on MBT-A and $[\text{MBT-A}]_2\text{Ni}^{2+}$ films. The current values were measured by STS during the process of actual lithographic patterning for each protruded patterns along the distance of 600 nm. The current values of MBT-A and $[\text{MBT-A}]_2\text{Ni}^{2+}$ films are about in the range of 1–4 and 1–5 nA in the threshold voltage, respectively. Based on the mechanism of AFM anodization lithography on organic resist [8],

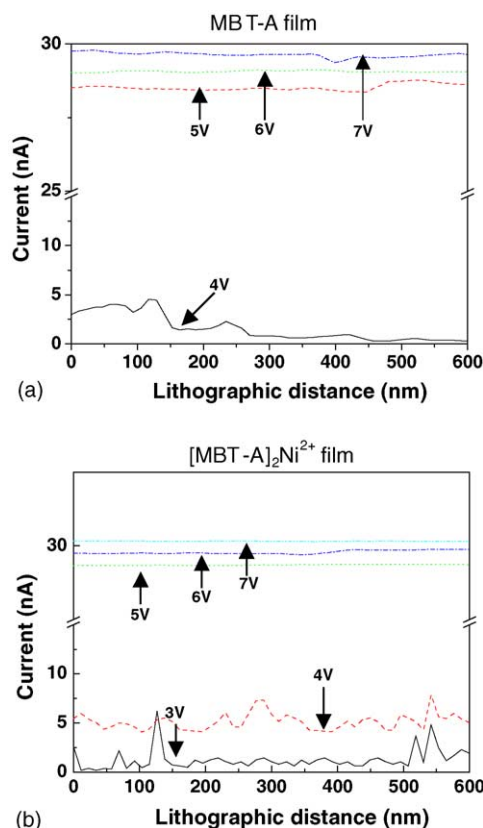


Fig. 4. Lithographic current profiles of protruded patterns under the various applied voltages.

it was confirmed that I – V curves of these films with low applied voltages showed very large fluctuation. It is suggested that the anodization lithography with low applied voltages is largely affected in organic materials on the surface. Thus, an organic resist, which has a small contact potential (V_0) like a $[\text{MBT-A}]_2\text{Ni}^{2+}$, has threshold voltage lower than that of a MBT-A film. Fig. 4 shows the change of current measured with lithographic distance from 5 to 7 V, too. The I – V curve was also formed during patterning of the lithographic

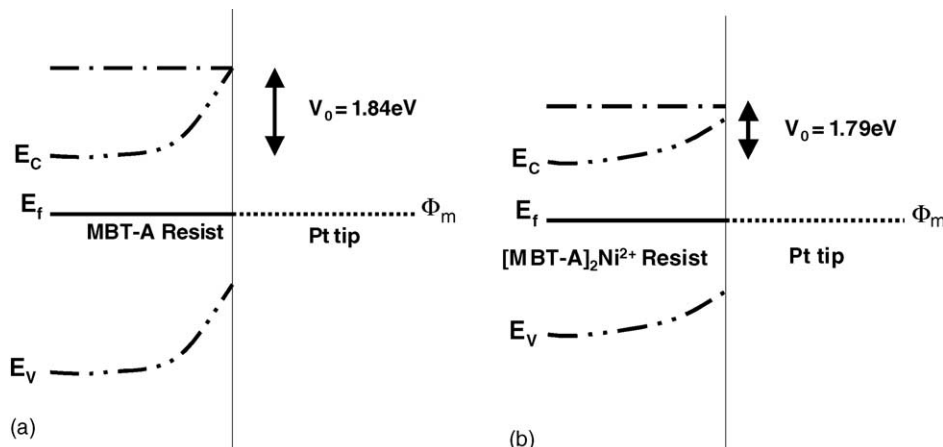


Fig. 3. Schematic band diagrams of AFM lithography system on (a) MBT-A and (b) $[\text{MBT-A}]_2\text{Ni}^{2+}$ films.

distance (600 nm). In various applied voltages ranging from 5 to 7 V, the measured current values of MBT-A and $[\text{MBT-A}]_2\text{Ni}^{2+}$ films were about 28.5–29.7 and 29.5–30.2 nA, respectively. It was observed that the current value of $[\text{MBT-A}]_2\text{Ni}^{2+}$ film was higher than that of MBT-A film at each applied voltages. So it was found that the current flow of $[\text{MBT-A}]_2\text{Ni}^{2+}$ film was better than that of MBT-A film. Also, it was suggested that contact potential (V_0) affects to the electric property of the organic film. A large fluctuation was not shown at high voltages, as against low voltage. Because the quantity of applied current between a tip and a sample is very large, the current in the reaction rarely affects the organic resist. Silicon oxide layers are protruded from momentarily current saturation.

The change of line width and line height is shown with the variation of applied voltages in Fig. 5. As shown in Fig. 5(a), the MBT-A and $[\text{MBT-A}]_2\text{Ni}^{2+}$ films do not show the large difference in the line width as increasing the applied voltage. It was reported that the change of line width in AFM lithography was affected by the wettability of surface, which can be changed by the functional groups of molecules [11]. However, in Fig. 5(b), it was observed the difference in the height as increasing applied voltages. And the line height of $[\text{MBT-A}]_2\text{Ni}^{2+}$ film was higher than that of a MBT-A film. From the result above, it was confirmed that the height of protruded pattern depends on the electrical property of molecular resist.

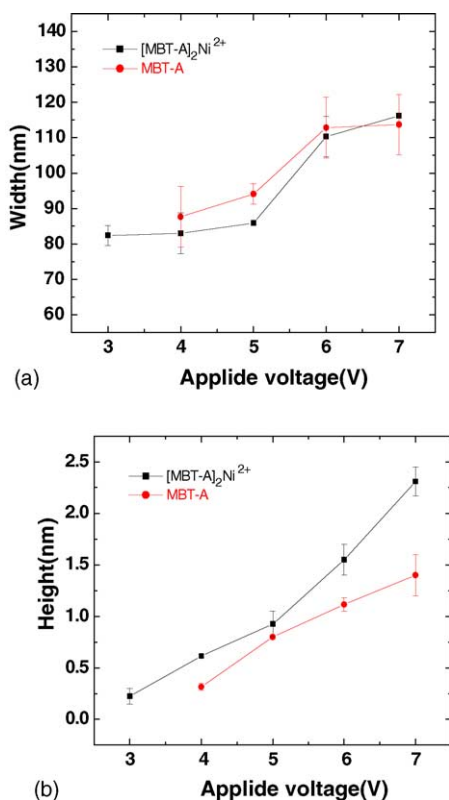


Fig. 5. Applied voltage dependence of (a) line width and (b) line height on anodization patterns of MBT-A and $[\text{MBT-A}]_2\text{Ni}^{2+}$ films.

4. Conclusion

The organic resist can be easily modified by the addition of specific functional groups and the property change of organic materials. Also, the use of the organic resists has an advantage of rapid lithographic scanning speed and optional pattern modification. The current quantity that flows between a tip and a sample affects not only largely in protruded patterns, but also the contact potential barrier of organic resist that is one of various lithographic factors. Therefore, it is very important to investigate the contact potential barrier of organic materials. From the results, the difference of contact potential barrier in organic resists affecting the threshold voltage and line height leads us to measure the current values on the organic resist during AFM anodization lithography.

Acknowledgements

This work was supported by the National Program for Tera-Level Nanodevices of the Ministry of Science and Technology as one of the 21st century Frontier Programs. Authors thank Sunkyung Kim for helpful discussions.

References

- [1] G.P. Lopez, H. Biebuyck, G.M. Whitesides, *Langmuir* 9 (1993) 1513.
- [2] S.Y. Chou, P.R. Krauss, P.J. Renstrom, *Science* 272 (1996) 85.
- [3] A. Dagata, J. Schneir, H.H. Harary, C.J. Evans, M.T. Postek, J. Bennett, *Appl. Phys. Lett.* 56 (1990) 2001.
- [4] W.B. Lee, E.R. Kim, H. Lee, *Langmuir* 18 (2002) 8375.
- [5] S.M. Kim, H. Lee, *J. Vac. Sci. Technol. B* 21 (2003) 2398.
- [6] S.M. Kim, S.J. Ahn, H. Lee, E.R. Kim, H. Lee, *Ultramicroscopy* 91 (2002) 165.
- [7] H.S. Lee, S.A. Kim, S.J. Ahn, H. Lee, *Appl. Phys. Lett.* 81 (2002) 138.
- [8] S.J. Ahn, Y.K. Jang, H.S. Lee, H. Lee, *Appl. Phys. Lett.* 80 (2002) 2592.
- [9] D. Stievenard, P.A. Fontaine, E. Dubois, *Appl. Phys. Lett.* 70 (1997) 3272.
- [10] P. Avouris, T. Hertel, R. Martel, *Appl. Phys. Lett.* 71 (1997) 285.
- [11] J.Y. Park, H. Lee, *Mater. Sci. Eng. C* 24 (2004) 315.
- [12] H. Sugimura, N. Nakagiri, *J. Vac. Sci. Technol. A* 14 (1996) 1223.
- [13] H. Ikegami, K. Ohmori, H. Ikeda, H. Iwano, *Jpn. J. Appl. Phys.* 35 (1996) 1593.
- [14] K. Ohmori, S. Zaima, Y. Yasuda, *Appl. Surf. Sci.* 162 (2000) 395.
- [15] H. Moore, K. Pollack, R. Shashidhar, *J. Am. Chem. Soc.* 125 (2003) 3202.
- [16] H.Y. Park, E.R. Kim, D.J. Kim, H. Lee, *Bull. Chem. Soc. Jpn.* 75 (2002) 2067.
- [17] N. Perez-Murano, C. Martin, N. Barniol, J.A. Dagata, *Appl. Phys. Lett.* 82 (2003) 3086.
- [18] R.K. Workman, C.A. Peterson, D. Sarid, *Surf. Sci.* 423 (1999) 277.
- [19] H. Bubert, H. Jenett, *Surface and Thin Film Analysis*, Germany, 2002, (Chapter 2).
- [20] B.G. Streetman, *Solid State Electronic Devices*, vol. 5, USA, 2000, (Chapter 5).